Integration of Aerial Thermal Imaging and Deep Learning for Fault Detection in Photovoltaic Panels: A Study at Thinh Long Solar Power Plant

Nga Le*, Hau Vu†, Nuttapong Porntipworawech†, Supa Waisayarat†, Minh Doan*†‡
* Human-Centered Engineering, Fulbright University Vietnam, Ho Chi Minh City, Vietnam
† Super Energy Corporation Vietnam, Ho Chi Minh City, Vietnam
‡ minh.doan@fulbright.edu.vn

2024 International Conference on Smart Energy Systems and Technologies (SEST) | 979-8-3503-8649-3/24/$31.00 ©2024 IEEE | DOI: 10.1109/SEST61601.2024.10694452

***Abstract*—Conducting operation and maintenance (O&M) procedures on solar energy panels is essential to ensure their proper functioning and adherence to energy production target. Parts of these routines typically include identifying faulty photovoltaic (PV) panels and repairing or replacing them to ensure optimal performance and longevity of the plant. In this paper, we propose a hybrid approach that combines deep learning computer vision with thermal analysis for the detection of PV panels with defects using aerial thermal images captured by drones. Our method integrates panel segmentation based on the Mask Region-Based Convolutional Neural Network (Mask-RCNN) with temperature distribution analysis to achieve automatic fault detection. The proposed hybrid approach is applied to thermal images obtained from the Thinh Long solar power plant in Vietnam. Through validation on approximately 850 images, we demonstrate the effectiveness of our method in accurately identifying various types of defects in solar panels, including hot spot, faulty diode, and under-performing groups of panels in a string. Our method was applied to a 50 MW currently in operation power plant and the results showcase the potential of integrating deep learning and thermal imaging for proactive maintenance of solar energy systems. This research contributes to advancing the field of renewable energy by providing a reliable and efficient methodology for detecting and addressing issues in PV panels, ultimately enhancing the reliability and efficiency of solar power generation.**

***Index Terms*—photovoltaic, thermal imaging, Mask-RCNN, deep learning, solar energy**

I. Introduction

In late 2023, the solar energy industry achieved unprecedented global growth, marked by record installation volumes and low sale prices, as reported by Chase [1]. This surge prompted BloombergNEF to revise its photovoltaics (PV) build forecast for 2024 upwards to 413 GW. Contemporary solar power plants, comprising numerous PV modules, necessitate meticulous maintenance for optimal operation. Detecting defects in PV panels, whether arising during installation or operation, to repair or replace them is critical for maximizing power production and ensuring profitability. Thus, regular inspection of panels is imperative to identify and address any deficiencies promptly [2], [3].

The project is privately funded by Super Energy Corporation Vietnam. and traveling cost for the presenters is partly funded by the Fulbright University Vietnam Personal Development Fund.

A common method to detect faulty PV panels is the use of aerial thermal imaging. An IR camera is usually carried by manned or unmanned quad-copters to capture the increased temperature of the defects on a panel [4]–[12]. A solar power plant operates at an order of MW power output typically consists of tens of thousands of PV panels which results in a few thousands images in an image capturing campaign using unmanned aerial vehicles (UAVs). Multi methods have been proposed in the literature to automate the defect detection process including classic computer vision [4]–[10] as well as deep learning techniques [11]–[14].

In 2017, Grimaccia et al. demonstrated the use of drones equipped with various sensors for inspecting PV systems in Northern Italy, identifying a range of impactful defects [3]. Following this, in 2018, Addabbo emphasized the growing global reliance on PV plants and the need for effective inspection methods like drones to ensure performance and facilitate timely maintenance, highlighting their increasing importance in the sector [8]. Later in 2022, Bommes et al. introduced a sophisticated method to automatically localize PV modules within large-scale plants using drone-mounted infrared cameras and incremental structure-from-motion [14].

In terms of classic computer vision technique, separate study by Grimaccia et al. in 2017 developed an image post-processing tool for UAVs to detect defects in photovoltaic systems, demonstrating its efficacy on real plant data [4]. Also in 2017, Arenella et al. proposed a method for detecting hot spots in photovoltaic panels using a combination of color and model-based information from drone-captured thermal images, significantly reducing false positives and proving both effective and efficient [5]. Moving to 2018, Gallardo-Saavedra et al. emphasized the importance of spatial resolution in aerial thermographic inspections of PV plants in Spain, offering guidelines for optimal camera and lens configurations [6]. A year later, Niccolai et al. discussed the integration of UAVs with artificial intelligence for photovoltaic plant inspections, stressing the improved efficiency and quality of data over traditional methods, and highlighting ongoing challenges in the field [7]. Building on these advancements, in 2020, Carletti et al. introduced a model-based approach for detecting PV panels and local hot spots using a novel algorithm designed to run in real-time on an embedded system aboard UAVs. This method

also incorporates global hot spot detection through multi-frame analysis, enhancing anomaly detection accuracy [10].

Moving to the use of deep learning, Dunderdale et al. utilized VGG-16 and MobileNet, coupled with a feature-based approach, to identify defects in photovoltaic modules from thermal images in South Africa, showcasing cost-effective defect classification [11]. By 2021, Bommes et al. advanced the application of deep learning in PV inspections by developing a semi-automatic tool that utilizes a ResNet-50 model to extract and classify PV module anomalies from UAV thermographic videos, achieving over 90% accuracy and proving scalable across different PV plants [12]. In 2022, the same researchers tackled the challenge of domain variation in PV plant data by employing a ResNet-34 model in an unsupervised domain adaptation framework, which effectively detected faults across different datasets, showing robust performance and practical utility for real-world applications [13].

In this paper, we propose a method for the detection of faulty PV panels in a solar power plant. The method took advantage of the Mask-RCNN model published by Bommes et. al [12] to separate each individual panel from an aerial thermal image for further analysis. While a few deep learning models for panel segmentation were published in the literature, the one in [12] was chosen for its open-source nature and reliability. Fault detection was then conducted by determining anomaly in the temperature distribution on the surfaces of the individual panels as well as group of panels in a string.

This study distinguishes itself from prior research by integrating data directly sourced from an operational power plant, and by incorporating input from the plant's operators to automate an existing O&M process. Additionally, to the authors' knowledge, this represents the inaugural application of temperature field analysis for the detection of common faults in PV panels. Moreover, the work is the first phase of a bigger project to automate the fault detection process for panel maintenance. At the moment, a manual panel maintenance campaign at bigger solar power projects such as Loc Ninh in Binh Phuoc, Vietnam may take up to a couple of months to finish. A 550 MWp cluster of plants Loc Ninh 1, 2, and 3 consists of approximately 1 million panels and a manual maintenance campaign consumes tremendous human resources. Last but not least, previous works seem to focus on individual panels only other than performing analysis on a group of panels in a PV string.

II. Methodology

This section provides a step-by-step overview of the method. Starting with individual panel extraction by the Mask-RCNN model, the in-house developed program perform thermal analysis on each panel as well as for a series of panels in a string.

A. Panel segmentation

Thermal aerial images of solar power plants, as depicted in Fig. 1, often exhibit interference from sun reflections on the surroundings, resulting in considerable noise. This noise presents a significant obstacle for traditional image processing techniques in removing it and isolating individual panels effectively. Consequently, employing deep learning techniques becomes essential for accurately segmenting individual panels from the composite image, facilitating precise automatic thermal analysis.

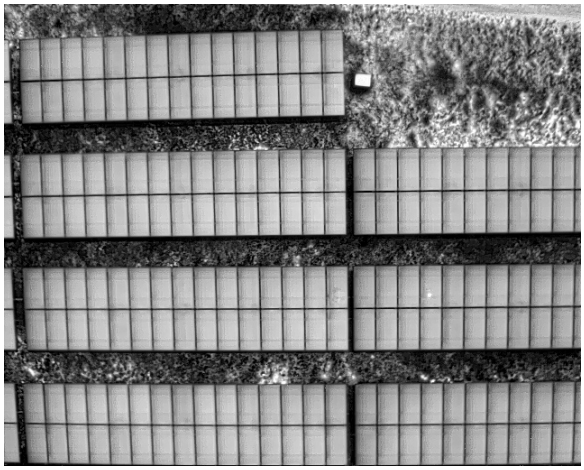

Fig. 1. Example of a raw thermal aerial image of the photovoltaic panels in a solar power plant.

The pre-trained weights for thermal images were retrieved from Bommes'PV Hawk repository [12]–[14] and integrated into the in-house developed program for panel segmentation. The segmentation model utilizes ResNet-50 as its backbone. Initially, it was trained for 59 epochs using weights pre-trained on the MS COCO dataset, with a learning rate of 0.001, momentum of 0.9, and a weight decay of 0.0001. Subsequently, the model underwent fine-tuning for an additional 60 epochs, during which the learning rate was lowered to 0.0001. According to Bommes et al., after fine-tuning, the Mask R-CNN model achieves an Average Precision (AP) of 90.01% and an F1-score of 90.51%. Specifically, at an Intersection over Union (IoU) threshold of 0.5, the AP significantly increases to 99.55%, and the F1-score reaches 98.92% [12].

The test data sets include picture captured by a DJI Matrice 300RTK vehicle carrying a Zenmuse H20T camera. According to the onboard GPS, all pictures were captured at approximately 75 m above sea level. The 50 MW solar power plant named Thinh Long is located in Phu Yen, Vietnam. Flying at that height, the IR camera can capture up to 8 rows and 25 columns of panels. The Mask-RCNN model with retrieved pre-trained weights has no difficulty in detection and extraction of whole PV panels in the images, as illustrated in Fig. 2. The deep learning model output the bounding box and group of detected pixels for each PV panel.

While segmentation using the pre-trained Mask-RCNN model can extract the panels accurately, the masks often include the gap between the panels as it can be seen in Fig. 4(a). These pixels of the gap sometimes consist of high temperature spots on the ground as shown in Fig. 3. To get rid of the gap, 3 adjacent pixels were removed from all the segmented images' boundaries as the pre-process.

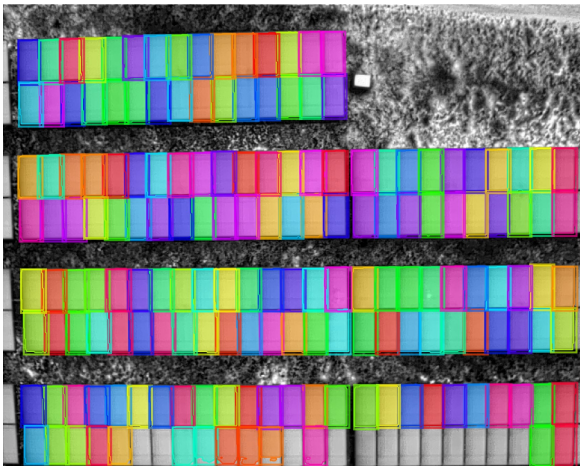

Fig. 2. Illustration of the panel detection and extraction process output using Mask-RCNN. The input is the image shown in Fig. 1.

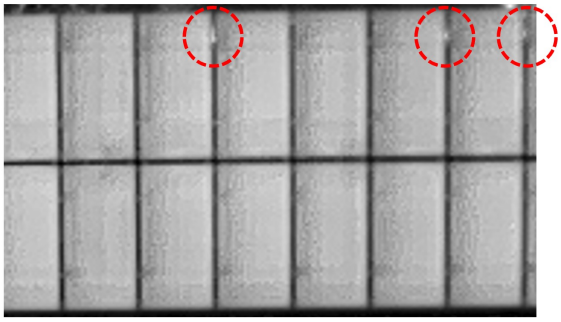

Fig. 3. Example of the high temperature spots on the ground, encircled in red between 2 consecutive panels.

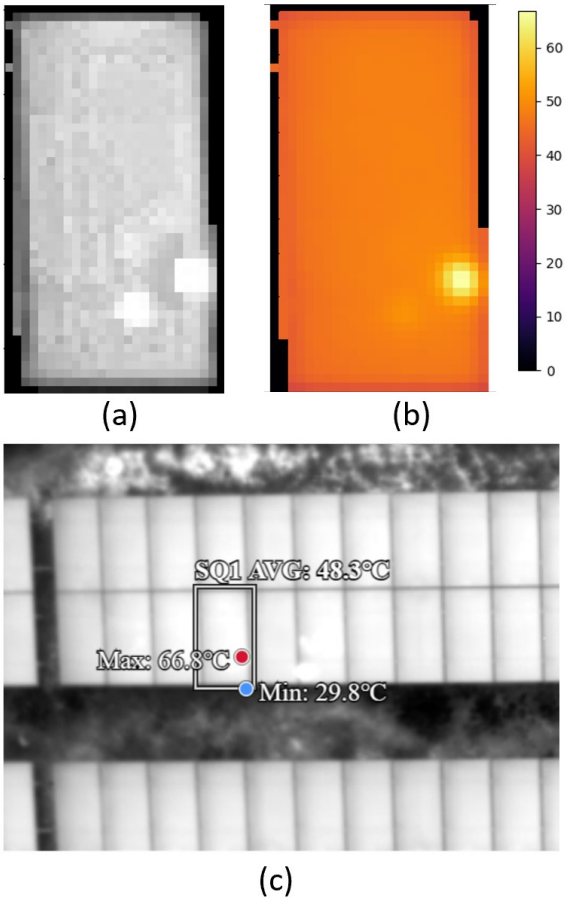

Fig. 4. Example of the Mask-RCNN model output of an individual panel (a), screenshot of the thermal analysis by DJI provided software namely DJI Thermal Analysis Tool (b), and output of the thermal analysis using DJI software development kit (c).

B. Individual panel thermal analysis

Once each individual panel is extracted out, temperature analysis was conducted to determine if the panel is normal or defective. Although transforming the IR images captured by the Zenmuse camera into temperature fields is not an open-source process, a software development kit (SDK) is available from DJI to call the process using any other program.

Each individual panel image was pre-processed, as described above, then input into the SDK to output its surface temperature. Fig. 4(a) shows an example of the output panel after extraction. The temperature data of each panel was then derived by the DJI's process. Fig. 4(b) and Fig. 4(c) verified that that the temperature output was similar between the DJI Thermal Analysis Tool and the process called by the SDK.

Classification of the fault was suggested by multiple studies in the literature. In this study, rules for hot-spot, cell, and diode defect were implemented as required by the power plant operator. Hot-spot can be detected by the temperature difference between the maximum and mean values. The mean temperature of a panel can go up to 50°C to 60°C in tropical countries as stated by Dhouib and Filali [15]. In reality, the average panel temperature at Thinh Long plant ranged from 40°C to 55°C. According to the operators, a nearby tree's shadow may raise a cell temperature by as low as 6°C while a surface crack may result in a 25°C higher than normal temperature. Therefore, hot-spot was classified when the maximum temperature is 15% higher than the mean.

The diode defect is commonly known to be easily detected by naked eyes as one-third or two-third of the panel is brighter than the rest on thermal images. The detection method follow the same approach. For the single/multi diode fault detection, pixels with temperature higher than 66.67%/33.33% compared with the rest were firstly separated as a mask. This mask was then evaluated if it spread out approximately 33.33% (for single faulty diode) and 66.67% (for multi faulty diodes) in the lateral direction. Additionally, this mask had to cover roughly 100% of the panel in the longitudinal direction.

C. String detection and analysis

Other than individual panel segmentation, detecting panels in strings is a crucial task to detect faulty strings and to map the faulty objects to the whole plant map. As the result from the Mask-RCNN model is not organized spatially, the initial step involves scanning through the model's results to identify the panel located centrally among all panels in the image. An

example of a typical thermal image from a survey is shown in Fig. 5, where the central panel refers to the one positioned at the center of the image. However, images capturing panels at the edges of a cluster, such as those shown in Fig. 6 and Fig. 10, require a different approach. Initially, the coordinates of the panels at the top-left and bottom-right are extracted from the Mask-RCNN output. Subsequently, the coordinates of the center of all panels, denoted as $x_{c,a}$ and $y_{c,a}$ are calculated by averaging the center coordinates of those 2 panels. The distance d_i from the center of each individual panel to the center of all panels is computed using

$$d_i = \sqrt{(x_{c,i} - x_{a,c})^2 + (y_{c,i} - y_{a,c})^2}, \tag{1}$$

where $x_{c,i}$ and $y_{c,i}$ represent the x and y coordinates of the center of each panel. The panel with the smallest value of d_i is then selected as the reference point for further analysis. Consequently, the program would look for panels aligned vertically and horizontally with the starting panel and label them in accordingly in the format (i, j) where i and j are the the row and and column index. Fig. 5 shows an example of this indexing process with the starting panel enclosed in blue. Once this process is done, the program check for adjacency of panels and perform temperature analysis on groups of panels.

The procedure to look for groups of panels starts with the upper left panel in a picture. The program detects the adjacent panels and assigns each group an unique ID number as shown in Fig. 6. Once a group of panels is identified, its average temperature can be calculated and compared with that of other groups.

III. Result and Discussion

The individual panel segmentation method was tested on 850 images and approximately 99% of the panels in the middle area of the images were detected successfully. Occasionally, panels near the edges of the images were not detected, as shown in Fig. 2. This only happens when the camera did not fully capture the whole panel. All the panels that were not captured by the pre-trained model had internal shorted circuits and would be discussed at the end of this section.

Fig. 7 gives an example of the input image and the detected 4 panels with high temperature spots. The maximum and mean temperature of the panels can be seen in Table. I. While the thermal image in Fig. 7(a) clearly shows that these 4 panels are defective and the average temperature in Table. I are consistent, the maximum temperature varies from 56.9°C to 85.6°C making the difference fluctuate between 24.2% to 77.6% of the mean, while the difference can be as low as 11.1°C. Therefore, the rule to detect a hot-spot was decided to be more than 15% of the mean temperature rather than considering the absolute temperature difference.

An example of the panel with single diode defect can be seen in Fig. 9. Using the method presented above, the high temperature mask, which is shown in Fig. 9(c), covered on average 98.9% in the longitudinal direction and 35.3% in the lateral direction.

TABLE I
THE MAXIMUM, MEAN TEMPERATURE, AND THEIR DIFFERENCE OF THE FAULTY PANELS IN FIG. 7.

Panel ID	Max Temp	Mean Temp	Difference
70	66.9°C	46.8°C	20.1°C
184	56.9°C	45.8°C	11.1°C
193	85.6°C	48.2°C	37.4°C
204	62.4°C	46.2°C	16.2°C

TABLE II
THE GROUP MEAN TEMPERATURE AND ITS DIFFERENCE COMPARED WITH THAT OF OTHER GROUPS IN FIG. 10.

Group ID	Mean Temp	Difference From Other Groups
1	34.4°C	9.2%
3	31.4°C	-3.4%
59	31.7°C	-2.2%
60	31.4°C	-3.38%

Lastly, the string fault detection is illustrated in Fig. 10 and Table II. The under-performing string with Group ID of 1 has an average temperature 9.2% higher than the rest of the panels. While performing analysis on the faulty strings, a limitation of the pre-trained model was exposed. In the case where multiple adjacent panels with internal shorted circuit making the whole string under-performing, the pre-trained model encountered difficulties segmenting those panels as shown in Fig. 11. Therefore, if the program only segmented and performed analyses on individual panels, those undetected panels with defects would be skipped. As they belong to a group of faulty panels which can be detected by the procedure, a technician will fortunately be aware of the undetected faulty panels by examine the raw image later in the maintenance process. Running on a common Dell Inspiron laptop, it took 9.3 s on average to perform all of the analyses on one image.

IV. Conclusion

This paper introduced an approach for detecting faulty PV panels in solar power plants, leveraging the Mask-RCNN model as presented by Bommes et al. (2021) for individual panel segmentation from aerial thermal images and analyzing temperature anomalies on both individual panels and groups of panels within a string. Our method effectively identifies faults, aiming to streamline the labor-intensive process of manual inspection of thermal images.

Future research will focus on rigorously evaluating the performance of our in-house developed code. This evaluation will involve a comprehensive comparison between the results obtained from our automated system and those derived from manual inspections. Additionally, we will compare our system's performance with that of other existing methodologies in the field.

Moreover, beyond its immediate application in fault detection, our method holds promise as a valuable data labeling tool for training future deep learning models. By automating the

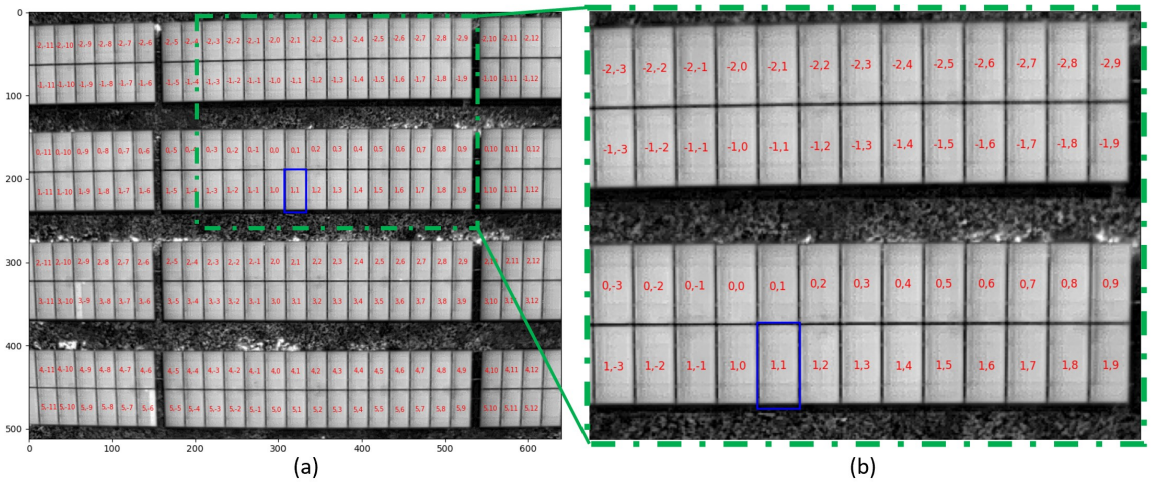

Fig. 5. Example of the panel indexing process. A zoom in picture (b) from the input image (a) shows the starting panel (1,1) enclosed in the blue rectangle.

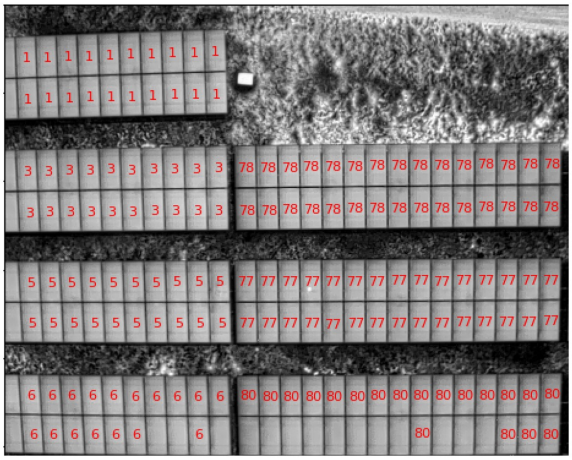

Fig. 6. Example of the panel group detection. Each group is given an unique ID number. The panels without ID were not detected by the pre-trained Mask-RCNN model.

process of labeling thermal images, the method contributes to the advancement of model training for improved performance and generalization.

ACKNOWLEDGMENT

Minh Doan would like to thank Mr. Hadi Ganjineh for his suggestion and vision on the project.

REFERENCES

[1] J. Chase, "Global PV Market Outlook, 4Q 2023," Solar, BloombergNEF, November 2023.

[2] M. Aghaei, F. Grimaccia, C. A. Gonano, and S. Leva, "Innovative Automated Control System for PV Fields Inspection and Remote Control," IEEE Transactions on Industrial Electronics, vol. 62, no. 11, pp. 7287-7296, 2015. DOI 10.1109/TIE.2015.2475235.

[3] F. Grimaccia, S. Leva, A. Dolara and M. Aghaei, "Survey on PV Modules' Common Faults After an O&M Flight Extensive Campaign Over Different Plants in Italy," in IEEE Journal of Photovoltaics, vol. 7, no. 3, pp. 810-816, May 2017, doi: 10.1109/JPHOTOV.2017.2674977.

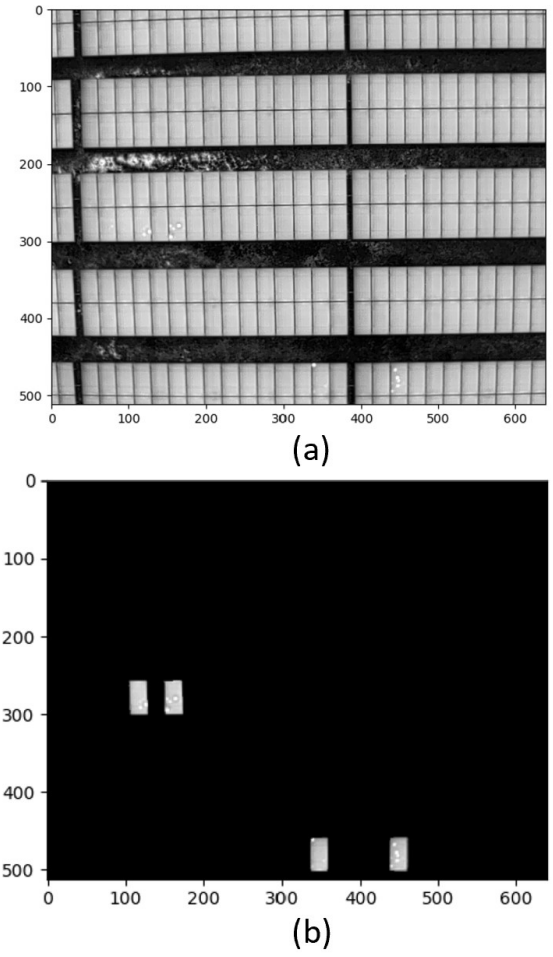

Fig. 7. Example of the input image (a) and the 4 faulty panels detected with high temperature.

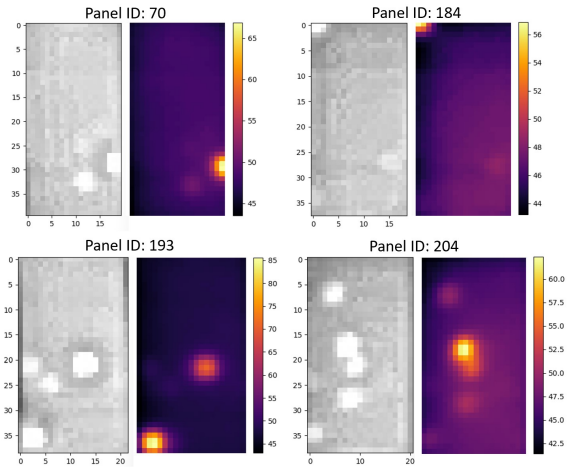

Fig. 8. Zoom-in images of the 4 faulty panels in Fig. 7 and Table. I with their temperature distribution.

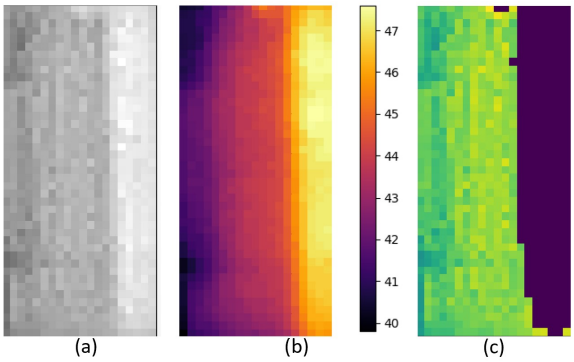

Fig. 9. Raw image (a) and temperature distribution (b) of a panel with the single-diode defect.

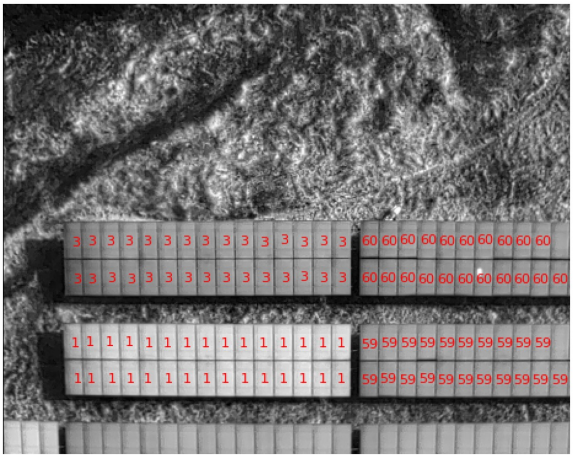

Fig. 10. Illustration of detecting groups of panels on a picture with an under-performing string.

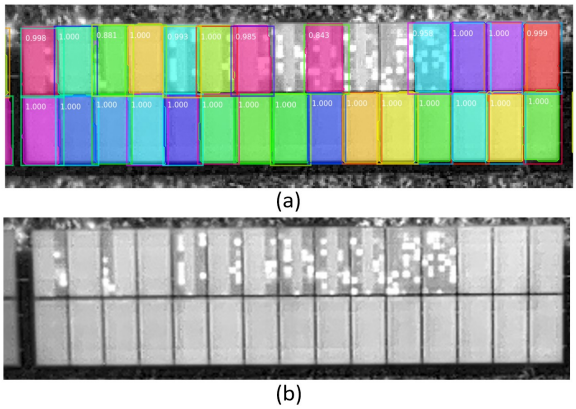

Fig. 11. Detection of panels in an under-performing string: the detected panels and scores by the Mask-RCNN model (a) and the raw image in the same field of view (b).

[4] F. Grimaccia, S. Leva, A. Niccolai, "PV plant digital mapping for modules' defects detection by unmanned aerial vehicles," J Ambient Intell Human Comput 11, 2027–2040, Jan. 2019, doi: 10.1007/s12652-019-01212-6.

[5] A., Arenella, A. Greco, A. Saggese, A., M. Vento, "Real Time Fault Detection in Photovoltaic Cells by Cameras on Drones," Image Analysis and Recognition (ICIAR), Lecture Notes in Computer Science, vol 10317, 2017, doi: , doi: 10.1007/978-3-319-59876-5_68.

[6] S. Gallardo-Saavedra, L. Hernández-Callejo and O. Duque-Perez, "Image Resolution Influence in Aerial Thermographic Inspections of Photovoltaic Plants," IEEE Transactions on Industrial Informatics, vol. 14, no. 12, pp. 5678-5686, Dec. 2018, doi: 10.1109/TII.2018.2865403.

[7] A. Niccolai, A. Gandelli, F. Grimaccia, R. Zich and S. Leva, "Overview on Photovoltaic Inspections Procedure by means of Unmanned Aerial Vehicles," 2019 IEEE Milan PowerTech, Milan, Italy, 2019, pp. 1-6, doi: 10.1109/PTC.2019.8810987.

[8] P. Addabbo, A. Angrisano, M. Bernardi, G. Gagliarde, A. Mennella, M. Nisi, S. Ull, "UAV system for photovoltaic plant inspection," IEEE Aerospace and Electronic Systems Magazine, vol. 33, no. 8, pp. 58-67, August 2018, doi: 10.1109/MAES.2018.170145.

[9] F. Grimaccia, S. Leva; A. Niccolai, "A semi-automated method for Defect Identification in large Photovoltaic power plants using Unmanned Aerial Vehicles," 2018 IEEE Power & Energy Society General Meeting (PESGM), Portland, OR, USA, 2018, pp. 1-5, doi: 10.1109/PESGM.2018.8586506.

[10] V. Carletti, A. Greco, A. Saggese, M. Vento, "An intelligent flying system for automatic detection of faults in photovoltaic plants," J Ambient Intell Human Comput, 11: 11, 2027–2040, Jan. 2020, doi: 10.1007/s12652-019-01212-6.

[11] C., Dunderdale, W., Brettenny, C., Clohessy, E.E., van Dyk, "Photovoltaic defect classification through thermal infrared imaging using a machine learning approach," Prog Photovolt Res Appl., 28: 177–188, Dec. 2019, doi: 10.1002/pip.3191.

[12] L. Bommes, T. Pickel, C. Buerhop-Lutz, J. Hauch, C. Brabec, IM. Peters, "Computer vision tool for detection, mapping, and fault classification of photovoltaics modules in aerial IR videos," Prog Photovolt Res Appl, 29(12): 1236-1251, Jul. 2021, doi: 10.1002/pip.3448.

[13] L. Bommes, M. Hoffmann, C. Buerhop-Lutz, T. Pickel, J. Hauch, C. Brabec, A. Maier, I. Peters, "Anomaly detection in IR images of PV modules using supervised contrastive learning," Progress in Photovoltaics: Research and Applications, vol. 30, no. 6, pp. 597–614, 2022, doi: 10.1002/pip.3518.

[14] L. Bommes, T. Pickel, C. Buerhop-Lutz, J. Hauch, C. Brabec, I. Peters, "Georeferencing of photovoltaic modules from aerial infrared videos using structure-from-motion," Progress in Photovoltaics: Research and Applications, vol. 30, no. 9, pp. 1122–1135, 2022, doi 10.1002/pip.3564.

[15] A. Dhouib, S. Filali, "Operating temperature of photovoltaic panels," Energy and the Environment, pp. 494-498, 1990, doi: 10.1016/B978-0-08-037539-7.50085-5.